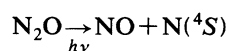
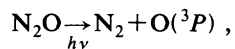


FIG. 2. Experimental setup for studies of radiative properties of free nitrogen atoms.

which was operated on (DCM) [4-(dicyanomethylene)-2-methyl-6-(*p*-dimethyl-aminostyryl)-4H-pyran] dye. The dye laser delivered pulses of tunable radiation of about 10-ns duration at a repetition rate of 10 Hz. The dye-laser radiation was frequency doubled in a KDP (potassium dihydrogen phosphate) crystal and tripled by mixing of the doubled frequency and the fundamental frequency in a BBO ( $\beta$  barium borate) crystal. In order to achieve the process, a mechanically compressed crystalline-quartz plate was used to rotate the fundamental and the doubled dye-laser radiation to obtain parallel polarization planes for the two waves before entering the BBO crystal. Starting with a dye-pulse energy of 50 mJ at 621 nm, we ended up with about 2 mJ at the 207-nm wavelengths required for two-photon excitation of the  $3p^4S_{3/2}$  state. The tripled frequency was isolated from the unwanted wavelengths by a Pellin-Broca prism and was subsequently sent into the experimental chamber which was filled with a low-pressure atmosphere of  $N_2O$ .

$N_2O$  was chosen because of its photophysical properties [8]. The processes



are energetically possible for wavelengths below 250 nm. The first of the two processes is the most efficient one dominating over the second, desired one, by a factor of 50 (Ref. [8]). The ground-state nitrogen atoms, created in the second process, find themselves two-photon resonant with the strong uv field.

In the experiments with a second-step excitation, an extra beam was diverted from the Nd:YAG laser to pump a Quanta-Ray PDL-1 dye laser operated with Rhodamin 6G or DCM dye to cover the wavelength regions 550–580 and 600–670 nm, respectively. The red laser light generated by the second dye laser was sent into the

experimental chamber close to and parallel with the uv beam. Inside the vacuum chamber the two beams were focused by an  $f=10$ -cm lens. Producing an overlap at the focus of the uv beam was simplified since the chromatic lens focused the uv light earlier than the visible light of the second-step beam. The detection of the fluorescence was made through a window perpendicular to the laser beam with a Hamamatsu R943-02 photomultiplier tube preceded by different interference filters. In the lifetime measurements, the signal was recorded by a Tektronix DSA 602 transient digitizer, while in the depletion spectroscopy a Stanford Research Instruments model 265 boxcar integrator was used. Both were connected to an IBM-compatible computer for data processing. When using the boxcar integrator, the intensity of the third-harmonic laser light was monitored with a diode in order to compensate for pulse-to-pulse fluctuations. Compensation for detector nonlinearities was made by a signal normalization routine used by Wolf and Tiemann [9]. Both boxcar integrator and transient digitizer were triggered by a diode, which detected a reflection of the red light from the first-step dye laser.

The vacuum chamber used for the experiments was cubic with a side of about 20 cm. After evacuation,  $N_2O$  could be introduced through a needle valve. The chamber was surrounded by coils for compensation of the earth's magnetic field. The gas pressure in the chamber was measured with a Pirani vacuum gauge, which was calibrated for  $N_2O$  in the pressure region of interest.

For depletion spectroscopy, calibration of the second-step dye laser was made by letting a beam reflection hit a neon-filled hollow-cathode lamp. When the wavelength coincided with certain neon transitions, a weak current transient was generated in the lamp discharge current. This signal could be sampled and used for wavelength calibration during a depletion-spectroscopy scan.

### III. MEASUREMENTS AND RESULTS

The correct tuning of the first excitation step laser (two-photon transition) was normally monitored by observing the near-ir fluorescence light from the platform state. In an early stage of the experiments, we tried to use the presence of stimulated emission on this line in the forward direction for ensuring correct tuning. Strong, stimulated emission was detected with a photodiode as has been reported in different investigations at this department [3], but only at gas pressures far too high for the experiments of interest in the present study. We also investigated the possibility of using the photoionization current expected when the platform states were two-photon resonant with the laser. Strong photoionization was detected using metal-plate electrodes close to the interaction volume, but, unfortunately, the atomic signal was mostly blurred by a nonresonant molecular background. This is a common problem in photoionization monitoring when not using a time-of-flight spectrometer or some other type of mass filter. Photoionization detection involves the presence of light scattering objects close to the interaction volume that are undesirable when detecting low levels of laser-induced fluorescence.

The  $3p^4S_{3/2}$  state was excited by two-photon absorption at 206.7 nm. Fluorescence was detected in the decay to the  $3s^4P_{5/2,3/2,1/2}$  states (742–747 nm) at pressures ranging from 0.05 to 0.5 mbar. The light from the decaying nitrogen atoms was averaged on the transient digitizer for multiple laser pulses. The decay constant was obtained by computer fitting of an exponential for times late enough to be outside the duration of the laser pulse. Under certain experimental conditions, more accurate data can be obtained by fitting a convolution of an exponential with a system response function to the experimental curve. However, such a method is not applicable in our case with multiphoton interaction and an unknown degree of saturation. The natural radiative lifetime unperturbed by collisions is obtained by linear extrapolation of the decay constants versus pressure to zero pressure. Normally, the collisional cross sections can be inferred from the slope of such Stern-Vollmer plots. This interpretation is not valid in our case. Using the previously described method for producing free atoms, several kinds of atoms, molecules, and ions are present in the interaction region. Hence, the collision partner of the nitrogen atoms is not well defined.

In corresponding measurements on the  $3p^4D_{7/2}$  state, the wavelength for two-photon absorption was 210.8 nm and fluorescence light was detected at 868 nm down to the  $3s^4P_{5/2}$  state. Decay curves for both investigated platform states are shown in Fig. 3. Several measurement series were taken and the corresponding Stern-Vollmer plots were constructed as shown in the lower part of Fig. 3. From the axis intercepts of the fitted lines, the radiative lifetimes were evaluated. The results are given in Table I, where the error bars include possible systematic errors as well as the statistical scattering in the data, resulting in an uncertainty in the extrapolation to zero pressure. Although other  $J$  components of the platform state were observed, only the state providing the strongest signal was selected for an accurate determination of the radiative lifetime.

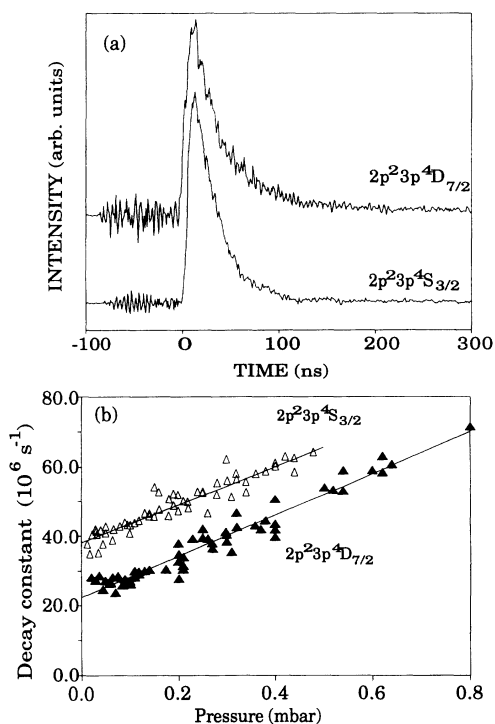


FIG. 3. (a) Experimental decay curves for the  $2p^2 3p^4 S$  and  $4D$  states reached by two-photon excitation. (b) Stern-Vollmer plots for the two states.

TABLE I. Natural radiative lifetimes of investigated nitrogen states.

State	Lifetime values (ns)		Theory
	This work	Other	
$2p^2 3p^4 D_{7/2}$	44(2)	43(3) <sup>a</sup> 27(3) <sup>b</sup> 53(8) <sup>c</sup>	37 <sup>d</sup>
$2p^2 3p^4 S_{3/2}$	26.0(1.5)	29(4) <sup>c</sup>	
$2p^2 6s^4 P_{5/2}$	41(7)		

<sup>a</sup>Reference [2].

<sup>b</sup>Reference [1].

<sup>c</sup>Reference [10].

<sup>d</sup>Reference [11].

Depletion spectra for transitions originating in the two platform states were recorded by scanning a second-step dye laser. By proper tuning of the first-step laser, well-defined fine-structure levels of the platform state could be selected. Every time the wavelength of the second-step laser coincided with a transition to an upper level,

Depletion spectra for transitions originating in the two platform states were recorded by scanning a second-step dye laser. By proper tuning of the first-step laser, well-defined fine-structure levels of the platform state could be selected. Every time the wavelength of the second-step laser coincided with a transition to an upper level,

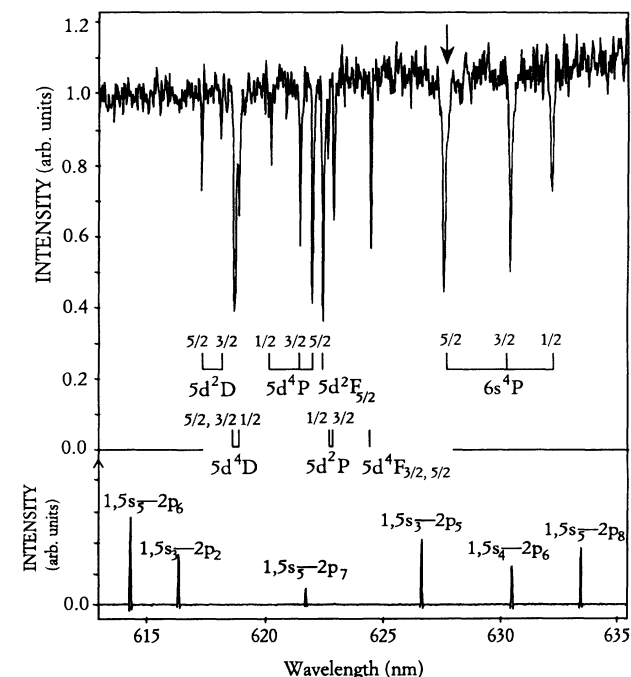


FIG. 4. Depletion spectra for nitrogen obtained by scanning a second-step dye laser inducing single-photon transitions from the  $2p^2 3p^4 S$  platform state, the population depletion of which is monitored on the 742-nm line. The lower part shows a neon spectrum with original Paschen notation.

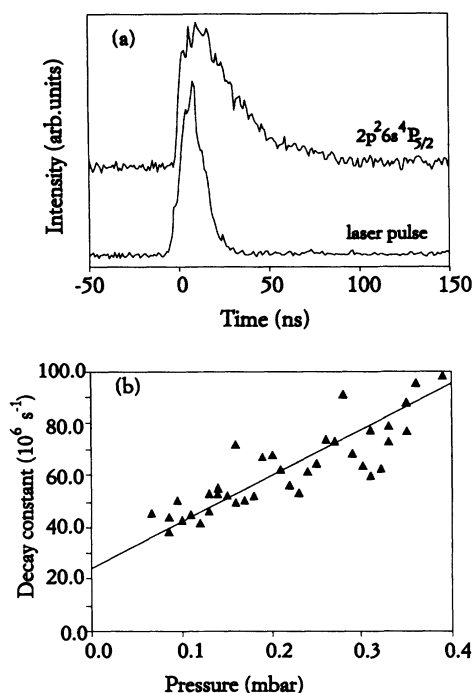


FIG. 5. (a) Experimental decay curve for the  $2p^2 6s^4 P$  state. A recording of the laser-pulse shape as detected in scattered stray light is included. (b) A Stern-Vollmer plot for the state, illustrating the evolution of the unperturbed lifetime value.

platform-state atoms were removed reducing the fluorescence intensity in the ir decay lines. In the studied wavelength regions, about 60 transitions were observed. All lines observed connect to states that are given with better accuracy from standard energy-level tables [7]. Our accuracy, largely limited by the laser linewidth and the wavelength calibration, is about  $3 \text{ cm}^{-1}$ . In Fig. 4, a depletion spectroscopy scan for lines originating in the  $3p^4 S_{3/2}$  state is shown together with optogalvanically recorded reference peaks from the neon discharge. It was noted that a very low laser power was needed to saturate the transitions. Some of the peaks in the figure show clear signs of saturation broadening.

In order to measure radiative lifetimes for states reached in the second excitation step, it is necessary to detect fluorescence light released in the decay of these states. A search revealed that sufficiently strong light

could only be detected from the  $5s$  and  $6s^4 P$  and the  $4d^4 D$  states, also considering spurious molecular fluorescence. Out of these states only the  $6s^4 P_{5/2}$  state was found to be long-lived enough to allow a reasonably accurate lifetime determination with the equipment used. This state was excited using the 627.7-nm line, marked with an arrow in Fig. 3. The decay was observed in the channel down to the  $3p^4 P$  state (581–583 nm). An experimental recording of the decay curve and a Stern-Vollmer plot for this state are shown in Fig. 5. From several such plots, a natural radiative lifetime of 41(7) ns was determined for this state. This value is included in Table I. It was noted that the slope of this plot was about three times larger than the ones for the lower, platform states, corresponding to the higher vulnerability to collisions for the more highly excited state.

#### IV. DISCUSSION

Apart from our newly determined experimental lifetime values, Table I also contains the available literature data. Our value for the  $3p^4 D_{7/2}$  state agrees with the revised value of Copeland *et al.* [2], but has a smaller error. Data from an emission-spectroscopy investigation by Richter [10] using a dc discharge allows a further lifetime value to be evaluated. That value is higher than our result. On the other hand, a theoretical calculation using the technique of Bates and Damgaard [11] yields a value lower than our experimental one. For the  $2p^2 3p^4 S_{3/2}$  state, a lifetime value from Richter's emission data can also be calculated. This value, although less accurate, agrees with ours within the mutual error bars. For the high-lying state, no literature data exist.

The techniques for free-atom production and stepwise laser excitation used in the present experiments on nitrogen can be used also for studying other light elements such as C, P, S, and Cl. In many cases a much more efficient atom production than in the present case can be expected because of more favorable photodissociation channels. The study of light elements as those mentioned is important to allow comparisons with theory and also because of their importance in many natural and man-induced processes.

#### ACKNOWLEDGMENT

This work was supported by the Swedish Natural Science Research Council.

- [1] W. K. Bischel, B. E. Perry, and D. R. Crosley, *Appl. Opt.* **21**, 1419 (1982).
- [2] C. A. Copeland, J. B. Jeffries, A. P. Hickman, and D. R. Crosley, *J. Chem. Phys.* **86**, 4876 (1987).
- [3] U. Westblom, S. Agrup, M. Aldén, and P. Cederbalk, *Appl. Opt.* **30**, 2990 (1991).
- [4] S. Agrup, U. Westblom, and M. Aldén, *Chem. Phys. Lett.* **170**, 406 (1990).
- [5] M. Aldén, H. Edner, P. Grafström, and S. Svanberg, *Opt. Commun.* **42**, 244 (1982).
- [6] S. Kröll, H. Lundberg, A. Persson, and S. Svanberg, *Phys. Rev. Lett.* **55**, 284 (1985).
- [7] S. Bashkin and J. Stoner, *Atomic Energy Levels and Grotrian Diagrams I* (North-Holland, Amsterdam, 1978).
- [8] H. Okabe, *Photochemistry of Small Molecules* (Wiley, New York, 1978).
- [9] U. Wolf and E. Tiemann, *Appl. Phys. B* **39**, 35 (1986).
- [10] J. Richter, *Z. Astrophys.* **51**, 177 (1961).
- [11] D. R. Bates and A. Damgaard, *Philos. Trans. R. Soc. London, Ser. A* **242**, 101 (1949).